Isolating the signal of ocean global warming

Isolating the signal of ocean global warming

M. D. Palmer,[1] K. Haines,[2] S. F. B. Tett,[3] and T. J. Ansell[1]

Received 17 August 2007; accepted 29 October 2007; published 6 December 2007.

[1] Identifying the signature of global warming in the world's oceans is challenging because low frequency circulation changes can dominate local temperature changes. The IPCC fourth assessment reported an average ocean heating rate of 0.21 ± 0.04 Wm^{-2} over the period 1961–2003, with considerable spatial, interannual and inter-decadal variability. We present a new analysis of millions of ocean temperature profiles designed to filter out local dynamical changes to give a more consistent view of the underlying warming. Time series of temperature anomaly for all waters warmer than 14°C show large reductions in interannual to inter-decadal variability and a more spatially uniform upper ocean warming trend (0.12 Wm^{-2} on average) than previous results. This new measure of ocean warming is also more robust to some sources of error in the ocean observing system. Our new analysis provides a useful addition for evaluation of coupled climate models, to the traditional fixed depth analyses.
Citation: Palmer, M. D., K. Haines, S. F. B. Tett, and T. J. Ansell (2007), Isolating the signal of ocean global warming, *Geophys. Res. Lett.*, *34*, L23610, doi:10.1029/2007GL031712.

1. Introduction

[2] The world oceans have a much larger heat capacity than other components of the climate system and it was recently estimated that, over the last 50 years, 84% of the stored heat energy of global warming has accumulated in the oceans [*Levitus et al.*, 2005] (hereinafter referred to as L05). It is difficult to make such calculations because the oceans do not warm uniformly across the globe [*Barnett et al.*, 2005] and the observed spatial and temporal coverage of subsurface temperatures is also very non-uniform [*AchutaRao et al.*, 2006]. Furthermore, ocean circulation can change on decadal timescales leading to convergence and divergence of heat which locally can be as large as the surface induced warming signal [*Barnett et al.*, 2005]. Attribution of ocean warming to anthropogenic forcings relies on using models to simulate the spatial variations in ocean heat content change with sufficient accuracy to provide a "fingerprint signal" [*Pierce et al.*, 2006]. However such signals cannot be easily reproduced in coupled general circulation models due to problems simulating the observed changes in large-scale surface pressure (and associated wind forcing [e.g., *Scaife et al.*, 2005; *Gillett et al.*, 2005]), the limited ocean model resolution, and the chaotic behaviour of the model atmosphere.

[1]Hadley Centre for Climate Change, Met Office, Exeter, UK.
[2]Environmental Systems Science Centre, Reading, UK.
[3]Department of Earth Science, University of Edinburgh, Edinburgh, UK.

0094-8276/07/2007GL031712

[3] We present a new analysis of the historical ocean observational temperature record which attempts to separate surface heat flux induced warming from advective warming, profile by profile, to generate a new metric of ocean temperature change. This analysis simplifies the spatial fingerprint of surface induced warming and provides a useful method for evaluating coupled climate models. Previous studies of the historical ocean thermal state have generally been based on thermal changes relative to fixed depths (e.g. the mean temperature above 300 m depth [*Levitus et al.*, 2000; *Ishii et al.*, 2003; *Willis et al.*, 2004; *Polyakov et al.*, 2005; L05; *Lyman et al.*, 2006]). Here we present decadal timescale analyses of the ocean thermal state relative to a fixed isotherm, 'isothermal analysis', following the work of *Walin* [1982], *Stevenson and Niiler* [1983] and *Toole et al.* [2004]. We do this because many dynamical phenomena (such as internal waves, mesoscale eddies or ocean circulation changes) modify the temperature distribution via vertical displacements of isotherms, but result in no gain or loss of heat by the ocean. These processes can cause large changes in mean temperature above a fixed depth, but are effectively filtered out in an isothermal analysis [*Stevenson and Niiler*, 1983; *Toole et al.*, 2004]. Therefore any changes to column-mean temperature bounded by an isotherm are more closely related to changes in air-sea heat fluxes than in a similar fixed depth analysis.

2. Data

[4] Our analyses are based on 7.4 million quality controlled ocean temperature profiles over the period 1956–2004 from the EN2 data set [*Ingleby and Huddleston*, 2007] of which approximately 7.0 million profiles come from the World Ocean Database 2001 (WOD01) [*Conkright et al.*, 2002]. Additional data sources include: the World Ocean Circulation Experiment (WOCE); the Bureau of Meteorology Research Centre (BMRC, Australia); the Commonwealth Scientific and Industrial Research Organisation (CSIRO, Australia); the Pacific Marine Environmental Laboratory (PMEL, USA); the Global Temperature-Salinity Profile Program (GTSPP, Australia, Canada, France, Germany, Japan, Russia); and the Argo profiling array [*Davis et al.*, 2001]. In the early 1990s GTSPP adds about 5% to the number of profiles used relative to WOD01, rising to about 10% in the late 1990s. Unlike WOD01, EN2 uses a time-evolving background field for the statistical background check, which is particularly useful for quality control of data in the tropical Pacific.

3. Method

[5] Each temperature profile for a given month is assigned to a 2° × 2° latitude-longitude grid box, and

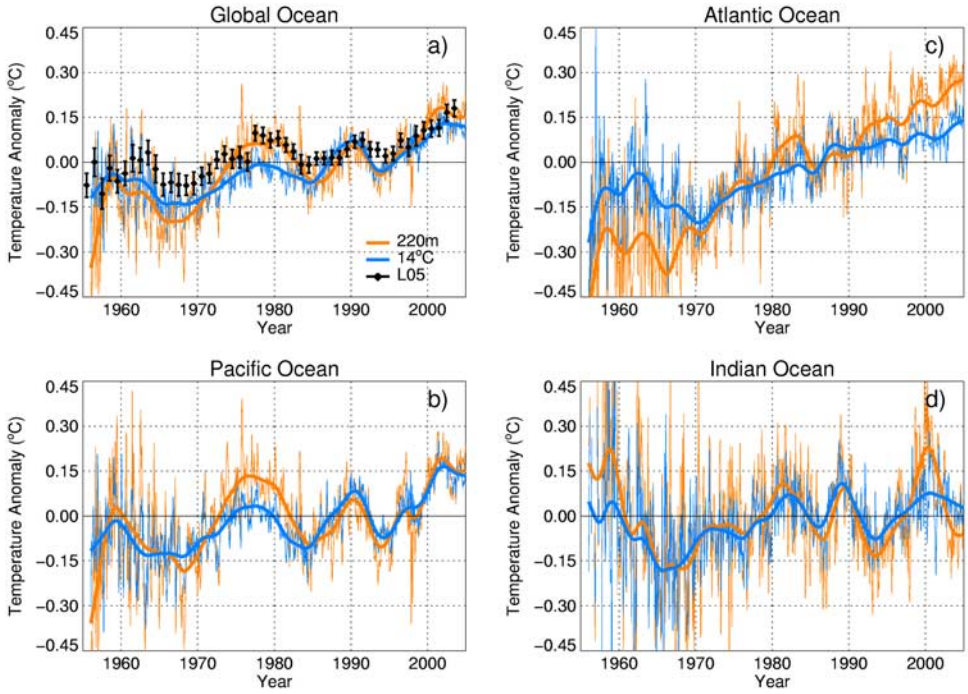

Figure 1. Time series of monthly mean temperature anomaly above the 14°C isotherm (blue) and 220 m (orange) for (a) Global Ocean, (b) Atlantic Ocean, (c) Pacific Ocean, and (d) Indian Ocean. The thick lines show these data after a 5-year low-pass filter has been applied. These data have been selected to have identical geographical coverage for the 14C and 220 m analyses. Also shown are the annual temperature anomalies with error bars (black) from L05 for the upper 300 m of the Global Ocean.

averages are formed from the available profiles to produce 588 monthly gridded fields of: (i) the mean temperature of the water warmer than 14°C, (ii) the depth of the 14°C isotherm, and (iii) the mean temperature of each profile down to 220 m. We choose the 14°C isotherm because it provides good coverage of the upper water column, at low to mid-latitudes, throughout the historical record, and 220 m because it is the overall time-spatial mean depth of the 14°C isotherm in low and mid-latitudes. We then produce a 12 month climatology based on the 49 years of data, and construct gridded anomaly fields to remove the seasonal cycle. Volume weighted temperature anomalies and area-weighted mean depth anomalies are then computed for the Globe, Atlantic, Pacific and Indian Oceans from each monthly field to produce time series.

[6] Grid boxes with no observations for a given month are not included in the computation (the implicit assumption is that all missing grid boxes have the area-weighted mean value of the observed grid boxes). For the first decade of observations between 2% and 10% of the total 2° × 2° grid boxes (relative to the area bounded by the 14°C outcrop) are sampled in each month, increasing to over 30% by the end of the time series. On average about 20% of the total grid boxes are sampled in each month, though this fraction is much higher in areas such as the North Atlantic. The analyses down to the 14°C isotherm and to 220 m fixed depth use identical grid box sampling for each month, to ensure that spatial coverage does not influence results. Where there is more than one occurrence of 14°C, due to a temperature inversion, we take the deepest occurrence. However, temperature inversions occur at only a few locations and our results are not sensitive to how they are treated.

[7] The time series are analysed to produce a trend and metrics of high and low frequency variability. A 5-year low-pass filter is applied to each monthly time series and we estimate the linear trend over the period 1956–2004 using a 'least squares' fit to the low-passed curve. The 'high frequency' variability is computed as the standard deviation of the monthly time series about the low pass filtered series, and the 'low frequency' variability is computed as the standard deviation of the low passed series about the linear trend.

[8] To evaluate the spatial coherence of the warming signals we produce trend estimates for anomalies in (i)–(iii) in each 2° × 2° grid box over the period 1965–2004. Following a similar approach to *Harrison and Carson* [2007], we divide the monthly temperature anomaly data into four decades (1965–1974, 1975–1984, 1985–1994 and 1995–2004) and only retain grid boxes that have at least 5 observations per decade. The coverage prior to 1965 is very poor, so we exclude these data in order to estimate trends over a larger number of grid boxes. The linear trend over the period 1965–2004 is then computed for each grid box.

4. Results

[9] Figure 1 shows the monthly and the 5-year low pass filtered mean temperature anomalies for all the water (i) warmer than 14°C, and (iii) above 220 m depth, for the globe and each ocean basin. We also show for comparison

Table 1. Summary Statistics Computed of Mean Temperature Above the 14°C Isotherm and the 220 m Depth in Each Ocean Basin[a]

	14°C Analyses			220 m Analyses		
Ocean Basin	HF Standard Deviation, °C	LF Standard Deviation, °C	Linear Trend, °C per dec.	HF Standard Deviation, °C	LF Standard Deviation, °C	Linear Trend, °C per dec.
Globe	0.046	0.042	0.043	0.077	0.065	0.061
Atlantic	0.078	0.045	0.059	0.12	0.052	0.13
Pacific	0.065	0.057	0.041	0.11	0.089	0.040
Indian	0.14	0.060	0.027	0.21	0.10	0.008

[a]The mean temperature trend, in °C per decade, for the 14°C and 220 m analyses; the high frequency (HF) standard deviations (computed from the residuals of the monthly and 5-year low-passed time series); and the low frequency (LF) standard deviations (computed from the residuals of the 5-year low-passed series and the linear fit), are shown.

the L05 results for the upper 300 m of the global ocean. There are some striking differences between the 14°C and 220 m analyses. There is a marked reduction in the high frequency variability of the 14°C temperature analyses over all ocean basins compared to the 220 m analyses. Much of this variability is likely associated with changing spatial sampling each month and the results imply that the mean temperature anomaly of waters warmer than 14°C is more robust to missing data than the 220 m analyses. At lower frequencies there is a reduction in multi-annual to decadal variability for the 14°C analyses, e.g. the reduced amplitude of the warm anomaly in the 1970s and 1980s in the Pacific and Global time series and the reduced multi-annual variability for the Atlantic and Indian time series throughout.

[10] Table 1 shows the high and low frequency standard deviations of the time series, and the linear trend for each basin. There is a 30–40% reduction in high frequency variability and a 25–40% reduction in low frequency variability of the 14°C analyses relative to the 220 m analyses. As well as a reduction in the monthly and multi-annual temperature variability, the 14°C analyses show a more uniform trend across the three ocean basins, with a global average of +0.043°C per decade. This is an indication that the reduced high and low frequency variability associated with dynamical effects allows a more uniform underlying signal to show through. In contrast, the 220 m trends differ between basins by up to an order of magnitude. The global trend in temperature for the 220 m analysis (+0.061°C per decade) is also about 50% larger compared to the 14°C analysis (Table 1). This difference mainly arises from the much larger trend in the Atlantic Ocean for the 220 m analysis; the trends for the Pacific basin being almost identical. Both 14°C and 220 m analyses show the largest high frequency variability in the Indian Ocean, which is the least well-observed basin and also has large seasonal circulation changes associated with the monsoon [*Schott and McCreary*, 2001]. We also find the largest low frequency variability occurs in the Pacific and Indian Oceans, as one would expect from the strong El Niño signal in these basins [*Krishnamurthy and Kirtman*, 2003; *McPhaden et al.*, 2006].

[11] Figure 2a shows a map of the July–August mean depth of the 14°C isotherm for the period 1956–2004. The deep areas of the subtropical gyres (>600 m in the North Atlantic) are areas where we expect changes in circulation might influence the isotherm depth on multi-annual time scales. Figures 2b, 2c, and 2d map the trends in mean temperature for waters warmer than 14°C, above 220 m, and trends in 14°C isotherm depth. The trends for the 14°C analysis shows more widespread warming than the 220 m analysis, and has a smaller range of trend values. The area weighted spatial variance about the mean trend is 0.67×10^{-2} and 1.6×10^{-2} (°C per decade)^2 for the 14°C and 220 m analyses, respectively. The 220 m mean temperature trends show similar spatial patterns to the work of *Harrison and Carson* [2007]: notably the warming along the west coast of the Americas; the bands of cooling around 40°N and in the equatorial Pacific; and the dominant warming in the North Atlantic. The regions of cooling are also broadly consistent with heat content trends for the upper 700 m, published in the IPCC fourth assessment report [*Bindoff et al.*, 2007]. The spatial pattern of the differences in temperature trends between the 14°C and 220 m analyses (not shown) has a correlation of 0.77 with trends in the 14°C isotherm depth (Figure 2d), which supports our hypothesis that locally, ocean temperature changes computed to a fixed depth are strongly influenced by dynamically induced changes in isotherm depth.

5. Discussion

[12] It is the reduction of both high and low frequency variability seen in the 14°C analysis time series (Figure 1) that allows the more uniform trends to emerge. In a fixed depth analysis contributions to high frequency variability arise from internal waves, mesoscale eddies and rapid variations in wind forced Ekman pumping [*Jayne and Marotzke*, 2001], while low frequency variations can arise from more prolonged Ekman pumping and changes in upper ocean circulation. The latter are often directly associated with changes in modes of atmospheric circulation [*Hurrell*, 1995; *McPhaden et al.*, 2006]. The potential for these phenomena to produce confounding signals in fixed depth estimates of ocean warming is a direct result of dynamical convergence and divergence of upper ocean waters and the coincident vertical heat advection across a fixed depth associated with these processes, combined with the inhomogeneous spatial and temporal observational record.

[13] The Pacific shows similar basin average warming trends of ~0.04°C per decade for the 14°C and 220 m analyses (Table 1). This is consistent with a redistribution of waters, associated with ocean circulation changes, being responsible for the greater inhomogeneity in the warming trend map for the 220 m fixed depth analysis (Figure 2c), but without substantial vertical net heat advection across 220 m in the regions sampled. In contrast the Atlantic 220 m analysis has a much greater warming trend than the 14°C analysis (Table 1). A possible explanation for the difference between these basins is related to the central role the

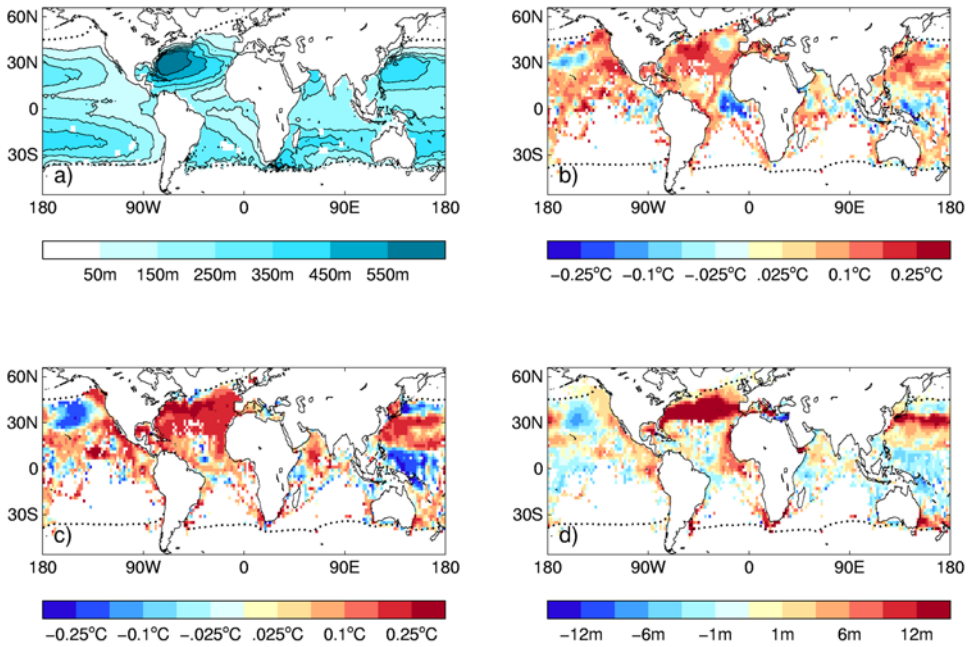

Figure 2. (a) The July–August–September mean depth of the 14°C isotherm over the period 1956–2004. (b) Trend (°C per decade) in mean temperature above the 14°C isotherm. (c) Trend (°C per decade) in mean temperature above 220 m. (d) Trend (m per decade) in depth (positive is deepening) of the 14°C isotherm. All trends are computed separately for each 2° × 2° grid box over the period 1965–2004. The trend data have been smoothed using a 1:2:1 grid box filter to remove some of the grid-scale noise. The dotted lines show the mean position of the 14°C outcrop line for August over the period 1956–2004 from HadISST [*Rayner et al.*, 2003].

Atlantic plays in the global thermohaline circulation (THC) [e.g., *Rahmstorf*, 2002], where warm waters are continuously imported from the rest of the world oceans. In a steady state these warm waters are transformed away but the considerable deepening trend of the isotherms in the North Atlantic (Figure 2d) suggests that this is a region of net heat accumulation over the period 1965–2004. The reduced warming above 14°C compared to the 220 m analysis (Table 1), is consistent with this explanation. Changes in wind patterns due to the North Atlantic Oscillation may have encouraged this build up of warm water and deepening of the 14°C isotherm in the North Atlantic subtropical gyre over several decades [*Leadbetter et al.*, 2007].

[14] Our 14°C analysis also provides some evidence that the net warm water convergence in the North Atlantic is accompanied by divergence elsewhere. The Indian Ocean warming is reduced in the 220 m analysis relative to the 14°C analysis (Table 1), suggesting export of >14°C water from the Indian Ocean over the period 1965–2004. Warm water export is also suggested by the dominance of shallowing trends in the 14°C depth (Figure 2d) in the subtropics of the Indo-Pacific. The small areas of 14°C deepening, e.g. in the South Indian Ocean, are in coastal regions dominated by dynamics and do not contribute much to the basin wide 14°C volume budget. We acknowledge that these inferences are limited by the poor observational sampling in the Indo-Pacific basins.

[15] The global trend in the 220 m mean temperature of +0.061°C per decade (≡0.17 Wm^{-2}) is 50% larger than the global trend in the 14°C isotherm analysis of +0.043°C per decade (≡0.12 Wm^{-2}). If the oceans had perfect sampling, these two quantities should be approximately the same because changing ocean dynamics would only redistribute heat. However, the historical observational sampling is extremely inhomogeneous and we suggest that this discrepancy could be an aliasing effect [*Gregory et al.*, 2004; *AchutaRao et al.*, 2006], caused by the relatively large number of observations in the North Atlantic (an area of heat convergence over the observational record), and relatively poorer sampling elsewhere, such as the Indian Ocean (areas of heat divergence over the observational record). In converting the 14°C mean temperature trend into a surface heat flux we have neglected any flux associated with mean deepening of the 14°C isotherm over time. However, we have argued that local depth trends (Figure 2d) primarily reflect dynamical convergence/divergence, we find no evidence for pervasive deepening. Given the biases in historical sampling, the flux term associated with 14°C deepening may be best estimated through modelling efforts.

[16] The L05 time series of annual temperature anomaly for the upper 300 m of the global ocean (Figure 1a) shows a linear trend of +0.032°C per decade (≡0.12 Wm^{-2}). Despite being a fixed depth analysis L05 is in close agreement with our 14°C analysis and is considerably reduced compared to our 220 m fixed depth analysis. The L05 analysis assumes a zero anomaly when observations are sparse [*Locarnini et al.*, 2006] while our analyses only uses sampled grid boxes in computing the time series. The L05 infilling with zero anomalies reduces the trend and amplitude of the time series [*Gouretski and Koltermann*, 2007; S. Gille, Decadal-scale temperature trends in the Southern Hemisphere ocean, submitted to *Journal of Climate*, 2007], which offsets the

sampling bias towards the heat convergence region of the N Atlantic. This appears to be a chance cancellation and the isothermal analysis presented here seems preferable in attributing local signal between dynamical convergence (isotherm deepening) and surface flux induced warming.

[17] Recently, biases among ocean observing platforms have been shown to influence global estimates of oceanic warming [*Gouretski and Koltermann*, 2007]. A large component of the historical observing array consists of expendable bathythermographs (XBTs) which are dropped into the water on a wire and measure temperature against depth assuming a known fall-rate. An additional advantage of our new analyses is that temperature above an isotherm is independent of the absolute reported depths, and therefore is independent of first-order errors in the fall-rate equation [*Hanawa et al.*, 1995]. The reduction of the 1970s and 1980s warm anomaly in our 14°C global time series is similar to recent XBT bias-corrected time series of global ocean temperature [*Gouretski and Koltermann*, 2007]. This raises the possibility that some of the reduction in low frequency variability for the isothermal analyses is the result of eliminating a source of bias in the observations.

6. Summary

[18] We have presented mean temperature changes above a fixed isotherm as an alternative to fixed depth analyses for ongoing assessment of the ocean thermal state. This new diagnostic is less prone to the influence of dynamical processes, at both high and low frequencies, and the results present a more globally uniform picture of ocean warming. Differences with a more widely used fixed depth analysis reveal important evidence of the global changes in warm water distributions over recent decades. In addition, calculation of mean temperature above a fixed isotherm eliminates some sources of bias in the historical observing array, which are problematic for fixed depth analyses. A limitation to our isothermal analyses is the exclusion of the high latitude oceans (where salinity plays a more important role in determining density). We suggest that our isothermal analyses provide a more accurate estimate of ocean thermodynamic changes over the twentieth century than pervious fixed depth analyses and a useful additional tool for assessing climate model response to greenhouse gas forcing.

[19] **Acknowledgments.** We thank Bruce Ingleby and Ruth Curry for help with processing the EN2 data and John Kennedy for supplying HadISST data. Thanks also to Greg Smith, Helene Banks and Sheila Stark for useful discussions on this work. The manuscript was improved following comments from two anonymous reviewers. This work was funded by: the UK Department for Environment, Food and Rural Affairs, the Government Meteorological Research and Development Programme, and the Natural Environment Research Council.

References

AchutaRao, K. M., B. D. Santer, P. J. Gleckler, K. E. Taylor, D. W. Pierce, T. P. Barnett, and T. M. L. Wigley (2006), Variability of ocean heat uptake: Reconciling observations and models, *J. Geophys. Res.*, *111*, C05019, doi:10.1029/2005JC003136.

Barnett, T. P., D. W. Pierce, K. M. AchutaRao, P. J. Glecker, B. D. Santer, J. M. Gregory, and W. M. Washington (2005), Penetration of human-induced warming into the world's oceans, *Science*, *309*, 284–287.

Bindoff, N. L., et al. (2007), in *Climate Change 2007: The Physical Science Basis. Contribution of Working Group I to the Fourth Assessment Report of the Intergovernmental Panel on Climate Change*, edited by S. D. Solomon et al., chap. 5, pp. 385–432, Cambridge Univ. Press, New York.

Conkright, M. E., et al. (2002), *World Ocean Database 2001*, vol. 1, *Introduction*, *NOAA Atlas NESDIS 42*, 159 pp., U.S. Gov. Print. Off., Washington D. C.

Davis, R. E., J. T. Sherman, and J. Dufour (2001), Profiling ALACEs and other advances in autonomous subsurface floats, *J. Atmos. Oceanic Technol.*, *18*, 982–993.

Gillett, N. P., R. J. Allan, and T. J. Ansell (2005), Detection of external influence on sea level pressure with a multi-model ensemble, *Geophys. Res. Lett.*, *32*, L19714, doi:10.1029/2005GL023640.

Gouretski, V., and K. P. Koltermann (2007), How much is the ocean really warming?, *Geophys. Res. Lett.*, *34*, L01610, doi:10.1029/2006GL027834.

Gregory, J. M., H. T. Banks, P. A. Stott, J. A. Lowe, and M. D. Palmer (2004), Simulated and observed decadal variability in ocean heat content, *Geophys. Res. Lett.*, *31*, L15312, doi:10.1029/2004GL020258.

Hanawa, K., P. Rual, R. Bailey, A. Sy, and M. Szabados (1995), A new depth-time equation for Sippican or TSK *T-7*, *T-6* and *T-4* expendable bathythermographs (XBT), *Deep Sea Res., Part I*, *42*, 1423–1451.

Harrison, D. E., and M. Carson (2007), Is the World Ocean warming? Upper-ocean temperature trends: 1950–2000, *J. Phys. Oceanogr.*, *37*, 174–187.

Hurrell, J. W. (1995), Decadal trends in the North Atlantic Oscillation: Regional temperatures and precipitation, *Science*, *269*, 676–679.

Ingleby, B., and M. Huddleston (2007), Quality control of ocean temperature and salinity profiles–historical and real time data, *J. Mar. Syst.*, *65*, 158–175.

Ishii, M., M. Kimoto, and M. Kachi (2003), Historical ocean subsurface temperature analysis with error estimates, *Mon. Weather Rev.*, *131*, 51–73.

Jayne, S. R., and J. Marotzke (2001), The dynamics of ocean heat transport variability, *Rev. Geophys.*, *39*, 385–412.

Krishnamurthy, V., and B. P. Kirtman (2003), Variability of the Indian Ocean: Relation to monsoon and ENSO, *Q. J. R. Meteorol. Soc.*, *129*, 1623–1646.

Leadbetter, S. J., R. G. Williams, E. L. McDonagh, and B. A. King (2007), A twenty year reversal in water mass trends in the subtropical North Atlantic, *Geophys. Res. Lett.*, *34*, L12608, doi:10.1029/2007GL029957.

Levitus, S., J. I. Antonov, T. P. Boyer, and C. Stephens (2000), Warming of the World Ocean, *Science*, *287*, 2225–2229.

Levitus, S., J. Antonov, and T. Boyer (2005), Warming of the World Ocean, 1955–2003, *Geophys. Res. Lett.*, *32*, L02604, doi:10.1029/2004GL021592.

Locarnini, R. A., A. V. Mishonov, J. I. Antonov, T. P. Boyer, and H. E. Garcia (2006), *World Ocean Atlas 2005*, vol. 1, *Temperature*, *NOAA Atlas NESDIS 61*, U.S. Gov. Print. Off., Washington, D. C.

Lyman, J. M., J. K. Willis, and G. C. Johnson (2006), Recent cooling of the upper ocean, *Geophys. Res. Lett.*, *33*, L18604, doi:10.1029/2006GL027033.

McPhaden, M. J., S. E. Zebiak, and M. H. Glantz (2006), ENSO as an integrating concept in Earth science, *Science*, *314*, 1740–1745.

Pierce, D. W., T. P. Barnett, K. AchutaRao, P. J. Glecker, J. M. Gregory, and W. M. Washington (2006), Anthropogenic warming of the oceans: Observations and model results, *J. Clim.*, *19*, 1873–1900.

Polyakov, I. V., U. S. Bhatt, H. L. Simmons, D. Walsh, J. E. Walsh, and X. Zhang (2005), Multidecadal variability of North Atlantic temperature and salinity during the twentieth century, *J. Clim.*, *18*, 4562–4581.

Rahmstorf, S. (2002), Ocean circulation and climate during the past 120,000 years, *Nature*, *419*, 207–214.

Rayner, N. A., D. E. Parker, E. B. Horton, C. K. Folland, L. V. Alexander, D. P. Rowell, E. C. Kent, and A. Kaplan (2003), Global analyses of sea surface temperature, sea ice, and night marine air temperature since the late nineteenth century, *J. Geophys. Res.*, *108*(D14), 4407, doi:10.1029/2002JD002670.

Scaife, A. A., J. R. Knight, G. K. Vallis, and C. K. Folland (2005), A stratospheric influence on the winter NAO and North Atlantic surface climate, *Geophys. Res. Lett.*, *32*, L18715, doi:10.1029/2005GL023226.

Schott, F. A., and J. P. McCreary (2001), The monsoon circulation of the Indian Ocean, *Prog. Oceanogr.*, *51*(1), 1–123.

Stevenson, J. W., and P. P. Niiler (1983), Upper ocean heat budget during the Hawaii-to-Tahiti shuttle experiment, *J. Phys. Oceanogr.*, *12*, 1894–1907.

Toole, J. M., H.-M. Zhang, and M. J. Caruso (2004), Time-dependent internal energy budgets of the tropical warm water pools, *J. Clim.*, *17*, 1398–1410.

Walin, G. (1982), On the relation between sea-surface heat flow and thermal circulation in the ocean, *Tellus*, *34*, 187–195.

Willis, J. K., D. Roemmich, and B. Cornuelle (2004), Interannual variability in upper ocean heat content, temperature, and thermosteric expansion on global scales, *J. Geophys. Res.*, *109*, C12036, doi:10.1029/2003JC002260.

T. J. Ansell and M. D. Palmer, Hadley Centre for Climate Change, Met Office, FitzRoy Road, Exeter EX1 3PB, UK. (matthew.palmer@metoffice.gov.uk)

K. Haines, Environmental Systems Science Centre, Harry Pitt Building, 3 Earley Gate, Whiteknights, Reading RG6 6AL, UK.

S. F. B. Tett, Department of Earth Science, University of Edinburgh, Grant Institute, The King's Buildings, West Mains Road, Edinburgh EH9 3JW, UK.